Abstract for the 20th Intl Workshop on Water Waves and Floating Bodies, Spitsbergen (Norway), May 29 - June 1, 2005

Wave-Body Interactions in a Two-Layer Fluid of Finite Water Depth

by Masashi KASHIWAGI

Research Institute for Applied Mechanics, Kyushu University
Kasuga, Fukuoka 816-8580, Japan, E-mail: *kashi@riam.kyushu-u.ac.jp*

1. Introduction

The fluid in ship hydrodynamics is mostly assumed to be of constant density. However, the density might change in special areas (a lake or an estuary) owing to variation in salinity and/or temperature of water. Another example of the density change is a thin layer of muddy water at the bottom of harbors or channels with relatively shallow water depth. These density changes may alter hydrodynamic characteristics of a ship, but little knowledge is available up to date. In the examples above, it is usually possible to model the fluid as a two-layer fluid in which a density discontinuity exists at the interface between the upper (lighter) and lower (denser) layers. The fluid in each layer may be assumed to be inviscid and incompressible with irrotational motion for the wave-body interaction problems.

The present paper is concerned with the boundary integral-equation (Green function) method, which directly solves the velocity potential on the wetted surface of a general body floating in a two-layer fluid with finite depth, and a body may intersect the interface as a general case. Numerical results are validated by checking theoretically proven hydrodynamic relations and by comparing with experiments which were carried out by realizing a two-layer fluid using water and isozole 300 (sort of iso-paraffin oil).

2. Formulation

A 2-D general body is assumed to straddle both of the upper and lower layers as a general case and to oscillate sinusoidally in response to an incident wave with circular frequency ω. The coordinate system and notations used in this paper are shown in Fig. 1. The free surface, the interface, and the water bottom are located at $z = 0$, $z = h_1$, and $z = h\,(= h_1 + h_2)$, respectively.

With the linearized potential-flow assumption, the velocity potential is introduced and defined in the form

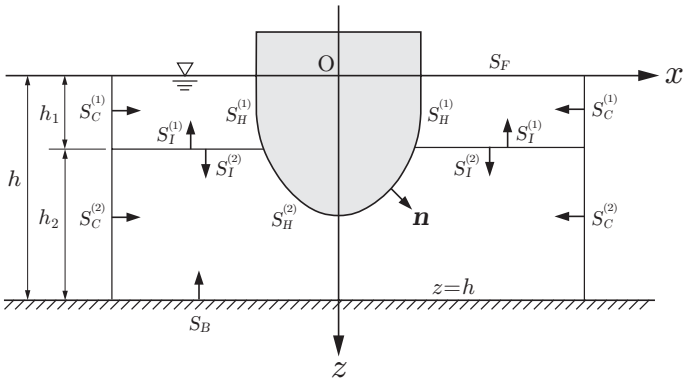

Fig. 1 Coordinate system and notations

$$\Phi^{(m)}(x,z,t) = \mathrm{Re}\Big[\,\phi^{(m)}(x,z)\,e^{i\omega t}\,\Big],\ m = 1, 2, \tag{1}$$

$$\phi^{(m)}(x,z) = \phi_0^{(m)}(x,z) + \phi_4^{(m)}(x,z) + \sum_{j=1}^{3} i\omega X_j\,\phi_j^{(m)}(x,z). \tag{2}$$

Here the superscript (m) denotes the fluid layer, with $m = 1$ and 2 corresponding to the upper and lower fluid layers, respectively. $\phi_0^{(m)}$ denotes the velocity potential of the incident wave, $\phi_4^{(m)}$ denotes the scattering velocity potential, and the sum of these will be denoted as $\phi_D^{(m)}$ and referred to as the diffraction potential. $\phi_j^{(m)}$ in (2) denotes the radiation potential with unit velocity in the j-th direction ($j = 1$ for sway, $j = 2$ for heave, and $j = 3$ for roll), and X_j denotes the complex amplitude of the j-th mode of motion, which may be determined by solving the motion equations of a body in waves.

The governing equation for these velocity potentials is the Laplace equation and the linearized boundary conditions to be satisfied are expressed as follows:

$$\frac{\partial \phi_j^{(1)}}{\partial z} + K\,\phi_j^{(1)} = 0 \quad \text{on } z = 0, \tag{3}$$

$$\frac{\partial \phi_j^{(1)}}{\partial z} = \frac{\partial \phi_j^{(2)}}{\partial z}, \quad \gamma\left(\frac{\partial \phi_j^{(1)}}{\partial z} + K\,\phi_j^{(1)}\right) = \frac{\partial \phi_j^{(2)}}{\partial z} + K\,\phi_j^{(2)} \quad \text{on } z = h_1, \tag{4}$$

$$\frac{\partial \phi_j^{(2)}}{\partial z} = 0 \quad \text{on } z = h\,(= h_1 + h_2), \tag{5}$$

$$\frac{\partial \phi_j^{(m)}}{\partial n} = n_j \ (j = 1 \sim 3), \quad \frac{\partial \phi_D^{(m)}}{\partial n} = 0 \quad \text{on } S_H^{(m)}, \tag{6}$$

where $K = \omega^2/g$, with g being the gravitational acceleration, $\gamma = \rho_1/\rho_2 \le 1$, with ρ_m being the density of the upper ($m = 1$) and lower ($m = 2$) fluids, and n_j denotes the j-th component of the outward normal vector (see Fig. 1). The parameter $\varepsilon = 1 - \gamma$, associated with the density ratio, will also be used, and for brevity the hyperbolic functions of $\cosh(x)$ and $\sinh(x)$ will be written as $\mathrm{ch}(x)$ and $\mathrm{sh}(x)$ hereafter.

3. Incident Wave Potential

The velocity potential of the incident wave incoming from the positive x-axis can be determined from (3)–(5) irrespective of the presence of a body, and the result may be expressed as

$$\phi_0^{(m)}(x,z) = \sum_{p=1}^{2} \frac{g\,a_p^{(p)}}{i\omega}\,\phi_{0p}^{(m)}(x,z), \tag{7}$$

$$\left.\begin{aligned} \phi_{01}^{(m)}(x,z) = Z^{(m)}(k_1 z)\,e^{ik_1 x}, \quad \phi_{02}^{(m)}(x,z) = \alpha(k_2)\,Z^{(m)}(k_2 z)\,e^{ik_2 x} \\ Z^{(1)}(kz) = \frac{k\,\mathrm{ch}kz - K\,\mathrm{sh}kz}{k}, \quad Z^{(2)}(kz) = \frac{K\,\mathrm{ch}kh_1 - k\,\mathrm{sh}kh_1}{k\,\mathrm{sh}kh_2}\,\mathrm{ch}k(z-h) \end{aligned}\right\} \tag{8}$$

where the wavenumber $k_p\,(p = 1, 2)$ in (8) satisfies the dispersion relation to be given from the boundary condition (4) on the interface, which can be expressed as

$$D(k) = K(k\,\mathrm{sh}kh - K\,\mathrm{ch}kh) + \varepsilon(K^2 - k^2)\,\mathrm{sh}kh_1\,\mathrm{sh}kh_2 = 0\,. \tag{9}$$

For a prescribed frequency K, there exist two solutions, and $k = k_1$ is referred to as the surface-wave mode (longer wavelength) and $k = k_2$ is referred to as the internal-wave mode (shorter wavelength).

In (7), the amplitudes of incident wave on the free surface and the interface are denoted as $a_p^{(1)}$ and $a_p^{(2)}$, respectively, for each of the k_p-wave mode. From the kinematic boundary condition, it can be shown that $a_p^{(1)}$ and $a_p^{(2)}$ are not independent and the following relation holds:

$$\frac{a_p^{(1)}}{a_p^{(2)}} = \frac{K}{K\,\mathrm{ch}k_p h_1 - k_p\,\mathrm{sh}k_p h_1} \equiv \alpha(k_p). \tag{10}$$

4. Numerical Solution Method

In this paper, the integral-equation method in terms of the Green function satisfying all homogeneous boundary conditions is employed to compute for a general case where an arbitrary-shaped body intersects the interface. The integral equation for the velocity potential on the wetted surface of a body can be derived by applying Green's theorem to each of the upper- and lower-layer fluids. With consideration of the interface boundary condition (4), the final result can be expressed in the form

$$C(\mathrm{P})\phi_j^{(m)}(\mathrm{P}) + \sum_{n=1}^{2}\int_{S_H^{(n)}} \phi_j^{(n)}(\mathrm{Q})\frac{\partial}{\partial n_\mathrm{Q}} G_n^{(m)}(\mathrm{P};\mathrm{Q})\,d\ell = \begin{cases} \displaystyle\sum_{n=1}^{2}\int_{S_H^{(n)}} \frac{\partial \phi_j^{(n)}(\mathrm{Q})}{\partial n_\mathrm{Q}} G_n^{(m)}(\mathrm{P};\mathrm{Q})\,d\ell & (j = 1 \sim 3) \\ \phi_{0p}^{(m)}(\mathrm{P}) & (j = Dp,\ p = 1, 2) \end{cases} \tag{11}$$

where $\mathrm{P} \equiv (x, z)$ and $\mathrm{Q} \equiv (\xi, \zeta)$ denote the field and integration points, respectively, on the body surface and $C(\mathrm{P})$ is the solid angle. $G_n^{(m)}(\mathrm{P};\mathrm{Q})$ represents the Green function, which has different forms depending on whether P and Q are in the upper or lower layer; details of which are shown in Ten & Kashiwagi (2004).

As a numerical solution method for (11), the so-called constant-panel collocation method is applied. In actual numerical computations, some additional field points are considered on both $z = 0$ (free surface) and $z = h_1$ (interface) inside the body to get rid of the irregular frequencies. The resultant over-constrained simultaneous equations are solved using the least-squares method.

5. Hydrodynamic and Restoring Forces

Once the velocity potentials on the body surface are determined, it is straightforward to compute the added-mass and damping coefficients in the radiation problem and the wave-exciting forces in the diffraction problem. The calculation formulae for these quantities are given as

$$A'_{ij} - i\,B'_{ij} = \frac{A_{ij}}{\rho_1 b^2 \epsilon_i \epsilon_j} - i\,\frac{B_{ij}}{\rho_1 \omega b^2 \epsilon_i \epsilon_j} = -\int_{S_H^{(1)}} \phi_j^{(1)} n_i\, d\ell - \frac{1}{\gamma}\int_{S_H^{(2)}} \phi_j^{(2)} n_i\, d\ell, \tag{12}$$

$$E'_{ip} = \frac{E_{ip}}{\rho_1 g a_p^{(p)} b \epsilon_i} = \int_{S_H^{(1)}} \phi_{Dp}^{(1)} n_i\, d\ell + \frac{1}{\gamma}\int_{S_H^{(2)}} \phi_{Dp}^{(2)} n_i\, d\ell, \tag{13}$$

where A_{ij} and B_{ij} are the added mass and the damping coefficient, respectively, in the i-th direction due to the j-th mode of motion, and E_{ip} is the wave-exciting force in the i-th direction induced by the incident wave of the k_p-wave mode. In nondimensional forms, $b = B/2$ denotes half the breadth at $z = 0$, and ϵ_j is defined as $\epsilon_1 = \epsilon_2 = 1$ and $\epsilon_3 = b$.

The hydrostatic restoring forces can be obtained by integrating the hydrostatic pressure over the wetted surface of an oscillating body. Gauss' theorem may be effectively used to each of the upper- and lower-layer region of the submerged portion of a body, and the coefficients of the restoring force in heave (C_{22}) and the restoring moment in roll (C_{33}) are summarized as

$$\left.\begin{aligned} C_{22} &= \rho_1 g B\Big(1 + \frac{\varepsilon}{\gamma}\frac{B_1}{B}\Big) \\ C_{33} &= \rho_1 g \mathcal{V}\,(-\overline{\mathrm{OB}} + \overline{\mathrm{BM}} + \overline{\mathrm{OG}}) \equiv \rho_1 g \mathcal{V}\,\overline{\mathrm{GM}} \end{aligned}\right\} \tag{14}$$

where

$$\mathcal{V} = V_1\Big(1 + \frac{1}{\gamma}\frac{V_2}{V_1}\Big), \quad \mathcal{V}\,\overline{\mathrm{OB}} = V_1 z_1 + \frac{1}{\gamma} V_2 z_2, \quad \mathcal{V}\,\overline{\mathrm{BM}} = \frac{B^3}{12}\Big(1 + \frac{\varepsilon}{\gamma}\frac{B_1^3}{B^3}\Big). \tag{15}$$

Here V_1 and V_2 are the submerged areas of a body in the upper- and lower-layer parts; the vertical positions of their are centers are denoted as z_1 and z_2; and B and B_1 are the breadths at $z = 0$ and $z = h_1$, respectively.

6. Radiated and Diffracted Waves at Far Field

The asymptotic form of the velocity potential as $|x| \to \infty$ may be obtained by substituting in (11) only the progressive wave terms of the Green function. The result is of the form

$$\phi_j^{(m)}(\mathrm{P}) \sim i\sum_{q=1}^{2} H_j^{\pm}(k_q)\, Z^{(m)}(k_q z)\, e^{\mp i k_q x} \quad \text{as } x \to \pm\infty. \tag{16}$$

Here $j = 1, 2, 3, 4p$, and $H_j^{\pm}(k_q)$ is called the Kochin function, which is defined as

$$H_j^{\pm}(k_q) = \begin{cases} \displaystyle\sum_{n=1}^{2}\int_{S_H^{(n)}} \Big\{\frac{\partial \phi_j^{(n)}}{\partial n} - \phi_j^{(n)}\frac{\partial}{\partial n}\Big\}\frac{W_n(k_q;\zeta)}{D'(k_q)}\, e^{\pm i k_q \xi}\, d\ell, & j = 1 \sim 3 \\ \displaystyle -\sum_{n=1}^{2}\int_{S_H^{(n)}} \phi_{Dp}^{(n)}\frac{\partial}{\partial n}\frac{W_n(k_q;\zeta)}{D'(k_q)}\, e^{\pm i k_q \xi}\, d\ell, & j = 4p \end{cases} \tag{17}$$

where

$$W_1(k;\zeta) = \gamma\,\alpha(k)\, k\, \mathrm{sh}kh_2\, Z^{(1)}(k\zeta), \quad W_2(k;\zeta) = \alpha(k)\, k\, \mathrm{sh}kh_2\, Z^{(2)}(k\zeta), \tag{18}$$

and $D'(k)$ denotes the derivative of (9) with respect to k.

In terms of (16), the elevation of progressive waves on the free surface ($z = 0$) and the interface ($z = h_1$) can be readily calculated, and the results are written as follows:

$$\eta^{(1)\pm}(x) \sim i\sum_{q=1}^{2}\sum_{p=1}^{2}\Big[a_p^{(p)} H_{4p}^{\pm}(k_q) - K\sum_{j=1}^{3} X_{jp} H_j^{\pm}(k_q)\Big] e^{\mp i k_q x} \quad \text{on } z = 0, \tag{19}$$

$$\eta^{(2)\pm}(x) \sim i\sum_{q=1}^{2}\sum_{p=1}^{2}\Big[a_p^{(p)} H_{4p}^{\pm}(k_q) - K\sum_{j=1}^{3} X_{jp} H_j^{\pm}(k_q)\Big] \frac{1}{\alpha(k_q)}\, e^{\mp i k_q x} \quad \text{on } z = h_1. \tag{20}$$

We can see from these that the relation (10) holds for the waves radiated and diffracted by a floating body, irrespective of the shape of a body. It is noteworthy for the diffraction problem that even when the incident wave contains only one wave mode (for instance $p = 1$), waves will be diffracted in two different wave modes ($q = 1$ and 2).

7. Experiments

To validate the numerical computation and to observe phenomena of wave-body interactions in a two-layer fluid, the experiments corresponding to the radiation and diffraction problems were conducted with a 2-D Lewis-form body which is of the half-breadth to draft ratio $H_0 = b/d = 0.833$ and the sectional area ratio $\sigma = A/Bd = 0.9$ ($b = B/2 = 0.1\,\mathrm{m}$ and $d = 0.12\,\mathrm{m}$). The two-layer fluid was realized by using isozole 300 for the upper-layer fluid (which is iso-paraffin oil with density $\rho_1 = 0.764\,\mathrm{g/cm^3}$ at 15°C) and water for the lower-layer fluid ($\rho_2 = 0.999\,\mathrm{g/cm^3}$ at 15°C). The size of the wave channel used in the experiment is 10 m in length, 0.3 m in breadth, and the depth of fluid (from the free surface to the bottom of the channel) is set equal to $h = 0.40\,\mathrm{m}$.

The depths of the upper and lower fluids were set in two different conditions: a) $h_1 = 0.060\,\mathrm{m}$, $h_2 = 0.340\,\mathrm{m}$ and b) $h_1 = 0.150\,\mathrm{m}$, $h_2 = 0.250\,\mathrm{m}$. It should be noted that a) corresponds to the case where a body intersects the interface, and b) corresponds to the case where a body floats only in the upper-layer fluid.

First, as the radiation problem, the forced heave oscillation test was carried out. In addition to the measurement of hydrodynamic forces, the radiated wave was also measured at $x/b = 10.875$ on the free surface and at $x/b = 9.860$ on the interface, using capacitance-type wave probes. In the experiment of the diffraction problem, we simply measured the incident wave and the wave forces in heave and sway on a fixed body.

With a video camera, measurement was also conducted for the wavelengths of generated waves on the free surface and the interface, which were confirmed to agree well with the one computed from the dispersion relation. However, it should be noted that the shorter wave of internal-wave mode tends to attenuate as it propagates.

8. Results and Discussion

Figure 2 shows the comparison of the amplitude of the wave radiated by the forced heave oscillation between measured and computed results for the case of $h_1 = 0.06\,\mathrm{m}$. The left figure is concerned with the value on the free surface and the right figure is the value on the interface. (Other results will be presented at the Workshop.)

It can be seen that the wave amplitude at a fixed position takes peaks and troughs depending on the frequency due to existence of both waves of surface-wave and internal-wave modes. Although the overall agreement is rather favorable, we can point out some of possible reasons of the discrepancy between the experiment and the numerical computation. First, measured results scatter due to the wave reflection from the longitudinal end of the wave channel, which was more prominent for the case of deeper upper layer, because the wave absorbing beach installed was not effective for waves on the deeper interface. Second, shorter waves tend to attenuate as they propagate, which was prominent in the internal-wave mode for almost all frequencies and in the surface-wave mode for higher frequencies. Last, the sensitivity of the wave probe used for measuring the elevation of isozole 300 (the free surface) was not perfect and also the surface elevation of isozole 300 was not exactly two dimensional (some transverse waves were observed). Nevertheless, qualitative tendency seems to be well accounted for by the present numerical computation based on the potential-flow assumption.

Reference

Ten, I and Kashiwagi, M (2004). "Hydrodynamics of a Body Floating in a Two-Layer Fluid of Finite Depth, Part-1: Radiation Problem", *J Marine Science & Technology*, Vol. 9, No. 3, pp. 127–141.

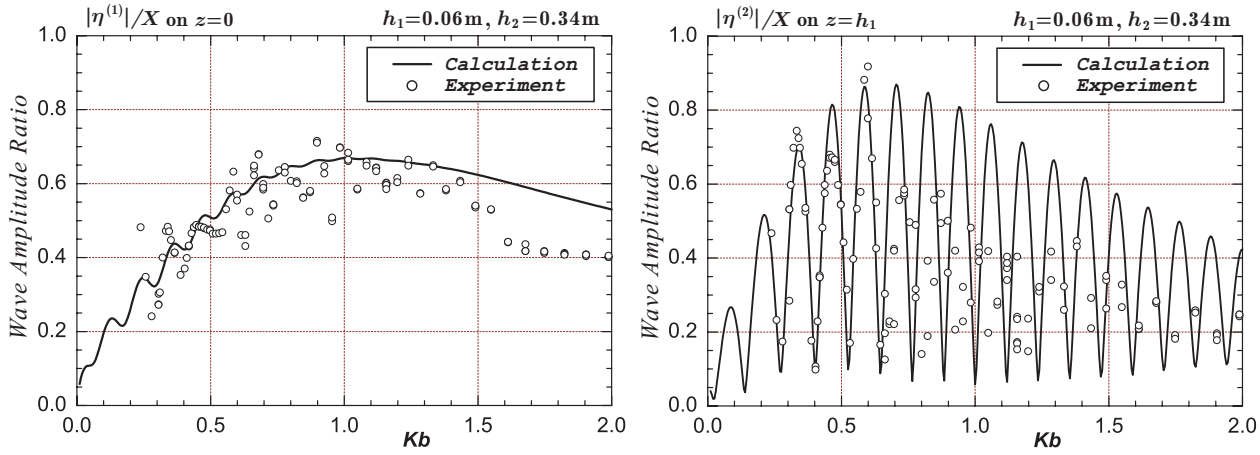

Fig. 2 Amplitude ratio of the wave on the free surface (left) and on the interface (right) radiated by forced heave oscillation; for $h_1 = 0.06\,\mathrm{m}$ and $h_2 = 0.34\,\mathrm{m}$.